Acta Chemica Scandinavica, 1997: 51: 585–592
Printed in UK – all rights reserved

ACTA
CHEMICA SCANDINAVICA
ISSN 0904–213X

Primary Free Radical Formation in Randomly Oriented DNA: EPR Spectroscopy at 245 GHz†

Barbara Weiland,[a] Jürgen Hüttermann[a,*] and Johan van Tol[b]

[a]Fachrichtung Biophysik und Physikalische Grundlagen der Medizin, Universität des Saarlandes, Klinikum Bau 76, 66421 Homburg/Saar, Germany and [b]Grenoble High Magnetic Field Laboratory-MPI-F/CNRS, BP 166, 38042 Grenoble Cedex 9, France

Weiland, B., Hüttermann, J. and van Tol, J., 1997. Primary Free Radical Formation in Randomly Oriented DNA: EPR Spectroscopy at 245 GHz. – Acta Chem. Scand. 51: 585–592. © Acta Chemica Scandinavica 1997.

245 GHz/8.7 T EPR spectroscopy has been applied for the first time to X-irradiated DNA equilibrated in different relative humidities and in frozen aqueous solution as well as to DNA components. Several primary and secondary radicals from nucleotides that are important with respect to DNA-located radicals could be isolated and simulated: the guanine cation, the cytosine anion, the thymine anion, the thymine H addition radical and the thymine allyl radical. The most clear-cut evidence for a DNA radical component was for the guanine cation, both the cytosine and the thymine anion being discernible. The guanine cation was found to be present in all DNA samples but was diminished in the frozen aqueous solutions. The contribution of the thymine anion decreased with increasing hydration level.

Over the past three decades long-standing and intense efforts have been made to try and unravel primary radical formation in DNA after irradiation with X-rays or heavy ions by electron paramagnetic resonance (EPR) spectroscopy (for a review see Refs. 1–3). DNA as a high molecular weight polymer with four different nucleotide subunits offers a large variety of potential sites for radical formation with, however, only few possibilities for component spectra separation at usual X-band frequencies (9.5 GHz). The typical fingerprint for structure determination in EPR of organic radicals, hyperfine interaction, is in general not sufficiently developed for separation in a randomly oriented specimen due to strong delocalization of the wavefunction. The other parameter, the *g*-tensor, also is of little value in this respect at X-band conditions; apart from rare cases such as alkoxyl-radicals in isolated nucleo-sides and -tides, the values deviate only little from the free electron *g*-factor.

Several attempts have been made to overcome this obstacle and to find physical conditions which allow for a reliable assignment of radical structures in DNA, a topic the significance of which is derived from the role of DNA as critical target in the context of cellular inactivation by ionizing radiation. One approach that comes to mind immediately is the application of high resolution EPR-derived techniques such as electron nuclear double resonance (ENDOR). We have tried this several times without success.[4] No structural but only matrix ENDOR was obtained probably due to extensive spin diffusion. No ENDOR studies from other laboratories have been reported.

Another approach was to employ oriented DNA fibers, pioneered by the work of Gräslund *et al.*[5] We have followed in the footsteps of these authors and initially gave support to their findings that led to what became known as the 'two component' model. This states that primary radical formation in DNA equilibrated at 76% relative humidity of D_2O involves selective formation of a cationic species on the guanine base ($\mathbf{G}^{\cdot+}$) and an anion on the base thymine ($\mathbf{T}^{\cdot-}$).[6] Using the same kind of samples but with specifically deuteriated thymine we showed subsequently that a third component should be involved making the thymine anion a minority species.[7] The chemical structure of this species is still under debate but arguments have been forwarded that it should be the anion on cytosine ($\mathbf{C}^{\cdot-}$).[8–11] More recently, by applying the new method of pulsed EPR in combination with continuous wave EPR we were able, using the same set of DNA samples as before, to assign several additional components. Apart from securing the previous ones and amending the previously undetermined parts of their spectral features it was possible to characterize, among others, a thymine allyl radical as additional species.[12]

For randomly oriented DNA samples, i.e., lyophilized

* To whom correspondence should be addressed.
† Lecture held at the 14th International Conference on Radical Ions, Uppsala, Sweden, July 1–5, 1996

powders and frozen aqueous solutions, the work of Gregoli and coworkers in the latter matrix gave rise to new results. Originally, the proposed mechanism was that, due to phase separation upon ice growth, free radical formation should follow what is termed the direct effect scheme. This implies that absorption of energy in the target molecule DNA takes place without connection to the processes in the polycrystalline ice phase. The role of the latter was thought to provide for reaction possibilities at higher temperatures giving secondary radicals involving the water matrix contributions.[13] This system and its mechanistic model was subsequently adopted by Symons and coworkers as well as Sevilla and coworkers. Concerning the primary radicals there was consensus that the two component model adopted originally by Gregoli also had to be expanded, like in the oriented fibers, by adding $\mathbf{C}^{\cdot -}$ as third component in frozen D_2O solutions of double-stranded DNA. The mechanistic picture was refined by adding a glass phase water shell in the immediate environment of DNA.[14,15] We have recently shed doubt on the validity of some of these assumptions. Specifically we ruled out the original Gregoli proposal of primary DNA-radicals only deriving from the direct effect. We invoked, from findings with electron scavengers, a strong contribution of electrons from the ice phase providing a source of anions by addition to DNA bases, explaining the large contribution of reduced species at 77 K.[16]

Fewer data have been presented on primary radicals in lyophilized samples of DNA. We have employed recently different amounts of water of hydration and found that there is a variation in spectral shape indicating different primary radical components.[17] Also, the contribution of hydration to the total radical yield in DNA[18,19] as well as to the radical yield of the only secondary radical, the thymine H addition species,[17] was found to be large.

It follows from the description given above that there is a strong need for indisputable assignments of primary radicals in DNA, specifically in randomly oriented samples (lyophilized powders of different hydration and frozen aqueous solutions). We report here on the first results obtained from the application of very high frequencies or fields (245 GHz, 8.7 T). In principle, the separation of minute differences in *g*-factors together with the lack of any forbidden transitions under these conditions would seem to make measurements at these frequencies an ideal tool to settle unambiguously the questions raised above. We have studied free radical formation in selected nucleotides and in DNA under different hydration conditions. The aim was to identify DNA radical components by comparison with nucleotide patterns.

Materials and methods

All nucleotides and DNA (as sodium salts from salmon testes) were purchased from Sigma and used without further purification. Samples in a deuteriated environment were dissolved in D_2O (99.8%, Merck) and freeze-dried twice. DNA was equilibrated at 15%, 35%, 45% and 76% relative humidity in desiccators containing oversaturated solutions of LiCl, $CaCl_2$, K_2CO_3 and NaCl in either H_2O or D_2O. Frozen aqueous solutions of DNA were prepared under a nitrogen atmosphere using 50 mg DNA per ml H_2O or D_2O. The low-temperature glass was produced using 7 M BeF_2 (Merck) in D_2O.

The samples were irradiated as compressed pellets of about 20 mg or small frozen cylinders of about 100 µl aqueous solution or 7 M BeF_2 glass, immersed in liquid nitrogen using X-rays (100 kV, 25 mA) with a dose of about 2×10^4 Gy. After storage and transport of the samples in liquid nitrogen the EPR measurements were performed within one week, at the 245 GHz spectrometer at the Grenoble High Magnetic Field Laboratory MPI-F/CNRS, which has been described previously.[20] Experiments at X-band frequencies were performed before and after storage in order to control the thermal stability of radicals during this time. Sample transfer to the cryostat led to an annealing temperature of about 90 K for a short time. Spectral analysis was performed using the software APOLLO.[21] In order to correct the signal for slight variations of the laser source intensity the output signal was normalized to the laser intensity measured simultaneously (Golay cell[20]). The field was calibrated by using Mn^{2+} as an internal standard, which can be found in all samples as an impurity. Its *g*-factor was determined to be 2.0010 by Q-band measurements compared with strong pitch ($g = 2.0028$).

Simulations were performed with the software SIMFONIA (Bruker, Karlsruhe).

Results and discussion

The three primary radical components mentioned above to be putatively present in irradiated DNA are located on the bases guanine, thymine and cytosine. The respective isolated nucleotide subunits, however, need not necessarily give spectra transferable to DNA. One has carefully to select the model compound and the matrix in order to establish conditions which potentially allow one to analyze the spectra from subunits relevant to the DNA situation. For the model compounds we chose 2′-deoxyguanosine 3′:5′-cyclic monophosphate (cdGMP), thymidine 5′-monophosphate (TMP) and 2′-deoxycytosine 5′-monophosphate (dCMP) (structures **I**, **II**, and **III**, respectively). The three radical components, the cation $\mathbf{G}^{\cdot +}$ and the two anions $\mathbf{T}^{\cdot -}$ and $\mathbf{C}^{\cdot -}$, are given as structures **IV**, **V** and **VI**, respectively. It has been shown that cdGMP offers the best conditions to study the guanine cation feature which relates to DNA.[22] In other guanine-containing complexes it is either not formed due to competition with other sites for oxidation (e.g., alkoxyl radical), not sufficiently stable or has a protonation state and corresponding spectral appearance

different from that from the DNA conditions.[23] Fig. 1 gives, on the left-hand side, the procedure for the isolation of a pattern which will be assigned subsequently to the $G^{\cdot+}$ in DNA. The top spectrum *A* is obtained from dry cdGMP powder upon measurement, without annealing, at 70 K. It has a strong feature in the center indicative of rhombic *g*-symmetry as well as some smaller outer lines. Some of the latter are due to manganese impurities which are used for *g*-factor calibration purposes. Annealing of the sample to about 200 K (spectrum *B*) results in the loss of the central feature without changing the manganese lines or other lines already present in *A*. Subtraction of *B* from *A* in the size given in the figure results in *C* which now mainly has only one species left. This feature is assigned to the $G^{\cdot+}$ radical on the basis of simulation, the data of which will be discussed below. The result of the simulation is shown as *D* for comparison. Note that the low-field line in *D* which corresponds to $g = 2.00438$ is, at the high field used, about 90 G apart from the free electron *g*-factor. In DNA this line will be used below as a marker for the presence of $G^{\cdot+}$.

Spectrum *B* mainly comprises features from the H

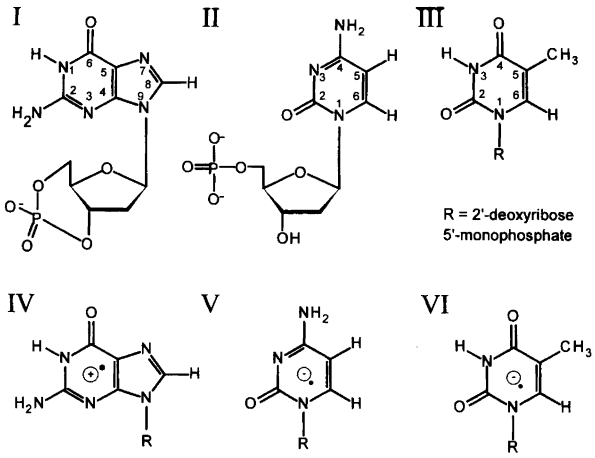

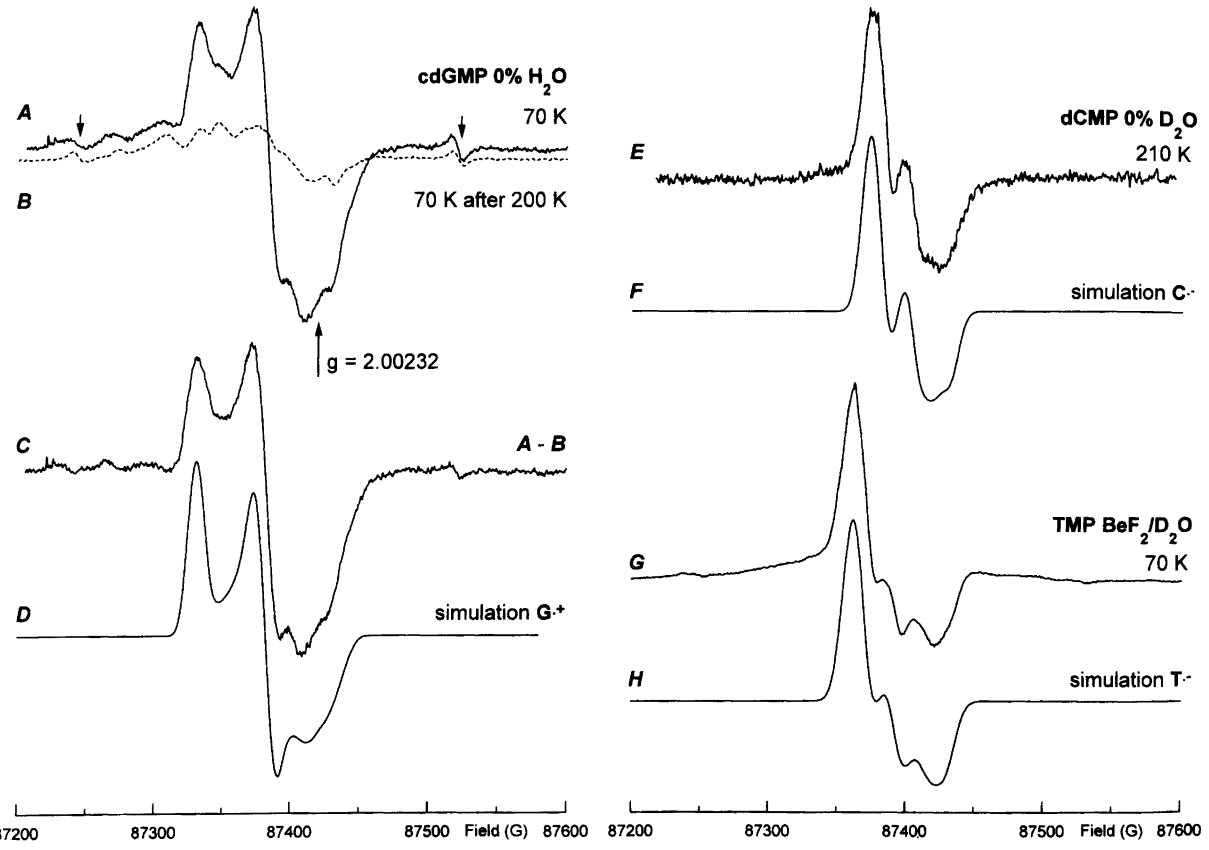

Fig. 1. ***A*** 245 GHz/8.7 T EPR spectrum of X-irradiated 2′-deoxyguanosine 3′:5′-cyclic monophosphate (cdGMP) as dry powder at a measurement temperature of 70 K. The outermost lines represent the first and fourth line of Mn^{2+} (marked by arrows). ***B*** The same as in ***A*** after warming to 200 K and recooling to 70 K. (The representation is reduced to the magnitude at which ***B*** was subtracted from ***A*** to give ***C***.) ***C*** Difference spectrum between ***A*** and ***B***. ***D*** Simulation of the guanine cation ($G^{\cdot+}$) using the data in Table 1. ***E*** 245 GHz/8.7 T EPR spectrum of X-irradiated 2′-deoxycytidine 5′-monophosphate (dCMP) in a dry environment after exchange of the water of crystallization with D_2O. The measurement temperature was 210 K. ***F*** Simulation of the cytosine anion ($C^{\cdot-}$) using the data in Table 1. ***G*** 245 GHz/8.7 T EPR spectrum of X-irradiated thymidine 5′-monophosphate (TMP) in a low-temperature glass of 0.1 M TMP in 7 M BeF_2–D_2O, recorded at 70 K. ***H*** Simulation of the thymine anion ($T^{\cdot-}$) using the data in Table 1.

addition radicals to carbon C8 of the guanine base which are probably mostly due to secondary reactions of the guanine anion that already occur at 77 K. These secondary radicals are also observed at 77 K in the dry nucleotide dGMP which does not stabilize the guanine cation as efficiently as cdGMP (data not shown).

The two patterns we associate with the pyrimidine anions are shown on the right-hand side of Fig. 1. Spectrum ***E*** is an experimental one from dCMP lyophilized from D_2O, measured at 210 K. This temperature was chosen because the oxidative products are much more pronounced at lower temperatures whereas the easily saturable anions dominate the spectra at higher temperature. The cytosine anion is most likely deuteriated but this small interaction need not be included in the simulation given as pattern ***F***.

Several attempts have to be made to obtain a spectrum of the thymine anion. In all powdered samples used there was too much overlap with secondary radicals. Eventually, the low-temperature glass BeF_2 was found to give very good results. Spectrum ***G*** was obtained experimentally upon measurement at 70 K. It is slightly dispersive but still useful. The simulated $T^{\cdot -}$ feature shown in ***H*** is seen to align very well with the experimental pattern. The latter is expected to represent the one-electron reduced thymine base species considering the reaction mechanisms in the glass.[24] Note that the pattern of $T^{\cdot -}$ which is plotted normalized on the same field scale as that of $C^{\cdot -}$ has a g_{max}-feature clearly appearing at lower field values. This, incidentally, also holds when cytosine anions are produced in BeF_2 glass (data not shown) and thus is not an effect of the environment of the anions. It shows that very small differences in g-factors between the two patterns can be discerned at the very high frequencies. We shall return to this below.

Two other radicals relevant to DNA but not necessarily primary radicals were isolated which involve the thymine base. One is isolated from DNA equilibrated in 76% relative humidity measured after annealing to 200 K. Fig. 2 (left part, ***A***) shows the respective spectrum. Spectrum ***B*** is from the same DNA taken before annealing. The difference, ***C***, gives a multiline pattern which, after comparison with simulation ***D***, is seen to represent the high-field form of the most well known secondary DNA radical, the thymine H addition species

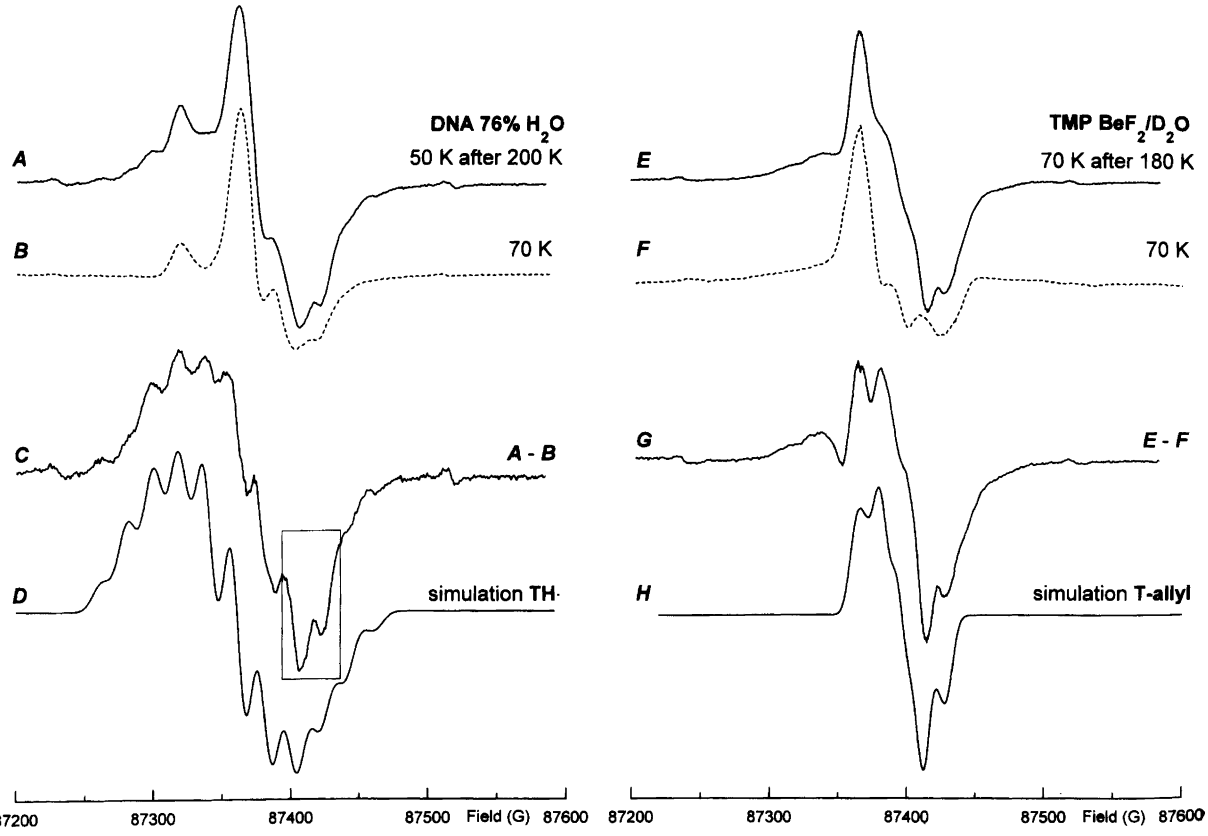

Fig. 2. ***A*** 245 GHz/8.7 T EPR spectrum of X-irradiated DNA equilibrated at 76% relative humidity in H_2O after annealing to 200 K and recooling to 50 K. ***B*** The same as in ***A*** but before annealing. (The representation is reduced to the magnitude at which ***B*** was subtracted from ***A*** to give ***C***.) ***C*** Difference spectra between ***A*** and ***B***. The marked region indicates a disturbance by a further component. ***D*** Simulation of the thymine H addition radical (TH˙) using the data in Table 1. ***E*** 245 GHz/8.7 T EPR spectrum of X-irradiated 0.1 M thymidine 5′-monophosphate (TMP) in 7 M BeF_2–D_2O at 70 K after warming to 180 K. ***F*** The same as in ***E*** but before annealing (cf. Fig. 1 ***G***), presentation reduced. ***G*** Difference spectra between ***A*** and ***B***, which gives mainly the thymine allyl radical. ***H*** Simulation of the thymine allyl radical (T-allyl) using the data in Table 1.

TH˙ (structure **VII**). Its 'octet' representation at X-band frequencies has now become eleven lines due to *g*-factor separation.

VII

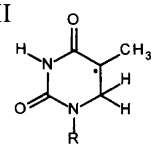

VIII

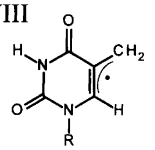

Comparison of the simulated with the difference spectrum shows that recording ***C*** of Fig. 2 contains some disturbance in the right-hand part of the spectrum (region marked). This may be due to another thymine-based DNA radical, the allyl species (structure **VIII**). Partial isolation of its high-field pattern is achieved from annealing TMP in a BeF_2 low-temperature glass where it derives from ˙OD attack as delineated in the right-hand part of Fig. 2. The experimental spectrum ***E*** obtained after annealing to 180 K has changed with respect to the initial spectrum at 70 K (trace ***F***). The difference ***G***, although containing in its low-field part contributions from a mixture of H and D addition to the base, allows us to assume, by comparison with the respective simulation, that the allyl radical is present to a large extent in spectrum ***E***. As may be rationalized by comparison with spectrum ***C***, some of the allyl radical lines fit just in that part of the pattern where disturbances of the thymine H addition radical features can be assumed.

We are not able so far to assign isolated patterns from 2′-deoxyadenosine 5′-monophosphate (dAMP) to primary radicals and furthermore we did not find a significant contribution of them in DNA (data from dAMP not shown).

The simulation data for the five different radical components discussed are compiled in Table 1 and compared with previous data from X- and Q-band investigations. One notes that the guanine cation was known before to have the largest *g*-factor component of all putative primary base radicals. This is corroborated by the high field results. In general, there is only a very limited database for *g*-factors available from, e.g., single crystal studies at X-band, which can be transferred to simulations at very high fields. The technical possibilities for determining the *g*-factors and their errors directly under these conditions are presently limited. Nevertheless, we found five decimal places for simulations useful, but do not imply that the error is in the last of these. It is Δg that can be determined at high fields with an accuracy one order of magnitude better than that of the typical X-band field.

Consider now the spectra obtained from lyophilized DNA equilibrated in different degrees of relative humid-

Table 1. Simulation data for spectra of DNA constituent radicals.[a]

	Literature				This work			
Radical	Posn./*g*	1	2	3	Posn./*g*	*x*	*y*	*z*
Guanine	N3[b]	0	0	13.8	N3	0	2	11.8
cation	N10[b]	0	0	6.8	N10	0	1	5.8
	H(C8)[b]	−4	−8.6	−6.8	H(C8)	−6	−7.6	−5.8
					Lw	10	10	10
	g[b]	2.0043	2.0038	2.0021	*g*	2.00438	2.00319	2.00230
Cytosine	H(C6)[c]	−22.6	−7.32	−11.84	H(C6)	−22.6	−7.32	−11.84
anion					Lw	12	12	12
	g[d]	2.0039	2.0034	2.0028	*g*	2.00295	2.00335	2.00219
Thymine	H(C6)[e]	4.5	11.6	21.1	H(C6)	22	8	12
anion					Lw	14	14	14
	g[e]	2.0037	2.0022	2.0032	*g*	2.00320	2.00358	2.00220
Thymine	3 H(C7)[f]	20.5	20.5	20.5	3 H(C7)	20.5	20.5	20.5
H addition	H(C6)[g]	38.4	42.2	37.8	H (C6)	35.4	39.2	33.8
	H(C6)[g]	40.9	40.1	44.2	H (C6)	40.9	38.1	43.1
					Lw	13	13	13
	g[f]	2.0024	2.0030	2.0042	*g*	2.00280	2.00372	2.00420
Thymine	H(C6)[h]	−6.2	−9.0	−14.0	H(C6)	−14.0	−6.2	−9.0
allyl	H(C7)[h]	−7.7	16.0	−24.7	H(C7)	−24.7	−7.7	−16.0
	H(C7)[h]	−7.7	16.0	−24.7	H(C7)	−13.57	−18.83	−16.0
	dir. cos.[h]	0.809	0	−0.5877	*xy*	−8.08		
		0	1	0	Lw	9	9	9
		0.5877	0	0.809				
					g	2.00293	2.00318	2.00258

[a]Hyperfine splittings and linewidth (Lw) in gauss. [b]Voit, K. PhD-thesis, Universität Regensburg (1986). [c]Close, D. M. and Bernhard, W. A. *J. Chem. Phys. 70* (1979) 210. [d]Bernhard, W. A. *Personal communication.* [e]Bernhard, W. A. and Patrzalek, A. Z. *Radiat. Res. 117* (1989) 379. [f]Pruden, B., Snipes, W. and Gordy, W. *Proc. Natl. Acad. Sci. 53* (1965) 917. [g]Hole, E. O., Sagstuen, E., Nelson, W. H. and Close, M. *J. Phys. Chem. 95* (1991) 1494. [h]Oloff, H. PhD-thesis, Universität Regensburg (1981).

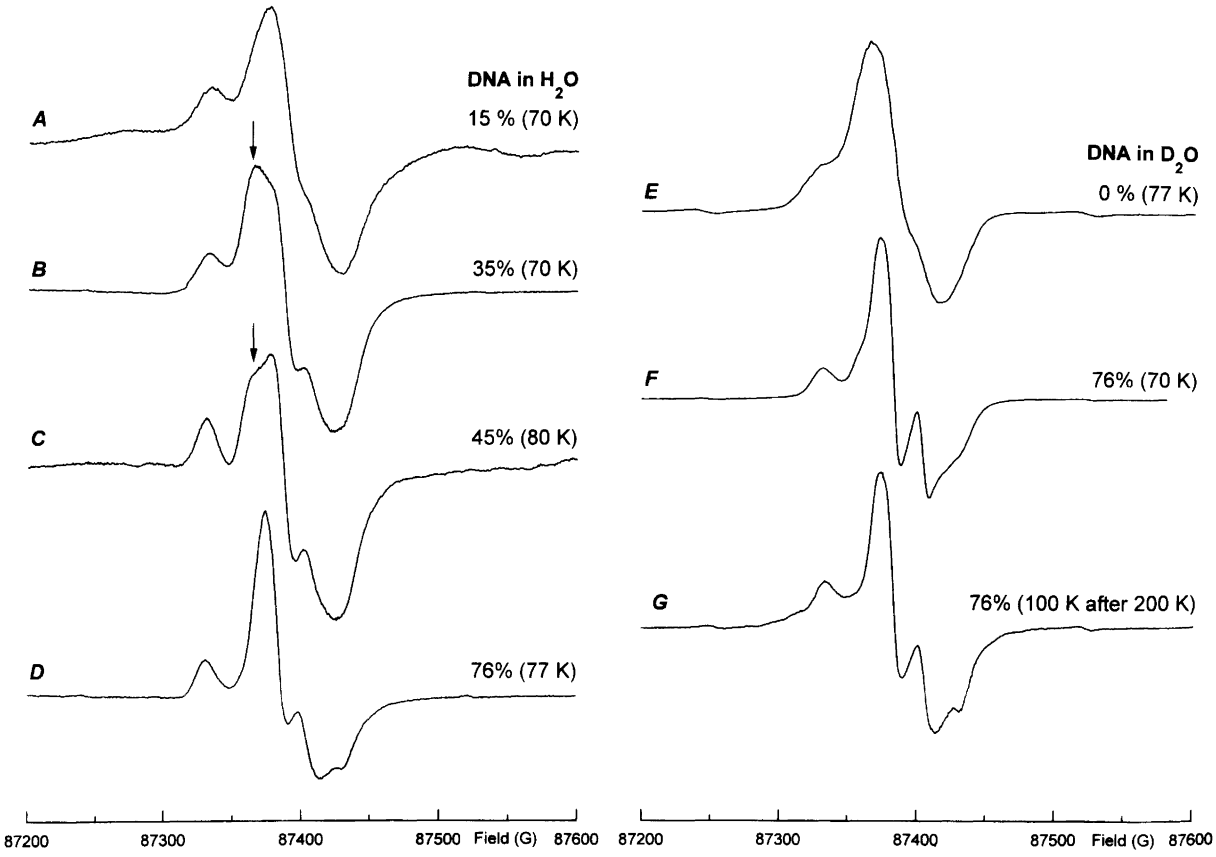

Fig. 3. 245 GHz/8.7 T EPR spectra of X-irradiated DNA equilibrated at increasing relative humidities in either H_2O or D_2O. ***A*** 15% H_2O; ***B*** 35% H_2O; ***C*** 45% H_2O; ***D*** 76% H_2O; ***E*** 0% D_2O; ***F*** 76% D_2O; ***G*** 76% D_2O after annealing to 200 K. The measurement temperatures are indicated in parentheses. The line disappearing at higher hydration levels is marked by arrows in ***B*** and ***C***.

ity over H_2O or D_2O vapour. The results are given in Fig. 3. Obviously the amount of water of hydration changes the spectra obtained under otherwise nearly identical conditions in both H_2O (traces ***A–D***) and D_2O (spectra ***E*** and ***F***). At first glance the resolution seems enhanced with increased water of hydration. A closer inspection is possible for the H_2O series which has more data. It reveals that the apparent gain in resolution in the spectrum, e.g., at 76% humidity, with respect at least to those at 35% and 45% humidity, comes from the loss or strong decrease of a component indicated by the disappearance of a line marked by arrows in spectra ***B*** and ***C***. We also note that the spectra for dry DNA in D_2O look very similar to the fairly dry (15% humidity) H_2O spectra. Furthermore, DNA in 76% D_2O after being warmed to 200 K (spectrum ***G***) is much more similar to the respective hydrated sample (cf. Fig. 2 ***A***) than at low temperature (spectra ***D*** and ***F***). Nevertheless, we are not yet able to isolate an additional component in spectrum ***G***.

The difference in spectra between different relative humidities in H_2O together with the simulated subunit species can be used as additional tools in reconstructing the DNA spectra from the components. Consider the left-hand part of Fig. 4. The top spectrum ***A*** is for 76% (spectrum ***D*** from Fig. 3). Spectrum ***B*** is a reconstruction using the simulated component spectra of Fig. 1. It is apparent that only $\mathbf{G}^{\cdot +}$ and $\mathbf{C}^{\cdot -}$ are needed in order to give a very good reproduction of the experimental pattern. Note, that we can make use of the D_2O-derived component of $\mathbf{C}^{\cdot -}$. Spectrum ***C*** repeats trace ***B*** from Fig. 3. If ***D*** is subtracted from ***C*** a feature is obtained that is given in spectrum ***E***. It has a remarkable similarity to the simulated pattern shown in Fig. 1 for the thymine anion for which the simulated spectrum is shown again as ***F*** for comparison. As stated above, there is a unique separation between the two anions due to the high *g*-separation capacity at these high fields. It is remarkable that the amount of the thymine anion decreases with increasing water content whereas the relative concentration of its putative successor, the thymine H addition radical (structure **VII**), is found to increase with hydration in DNA at elevated temperatures.[17]

Another feature which can be probed at high fields relates to the mechanisms of free radical formation from DNA in frozen aqueous solutions. We have mentioned above that these are the subject of debate with respect to direct effect mechanisms. The right-hand part of Fig. 4 gives two spectra in frozen H_2O and D_2O matrices, respectively. A more detailed analysis of the spectra is

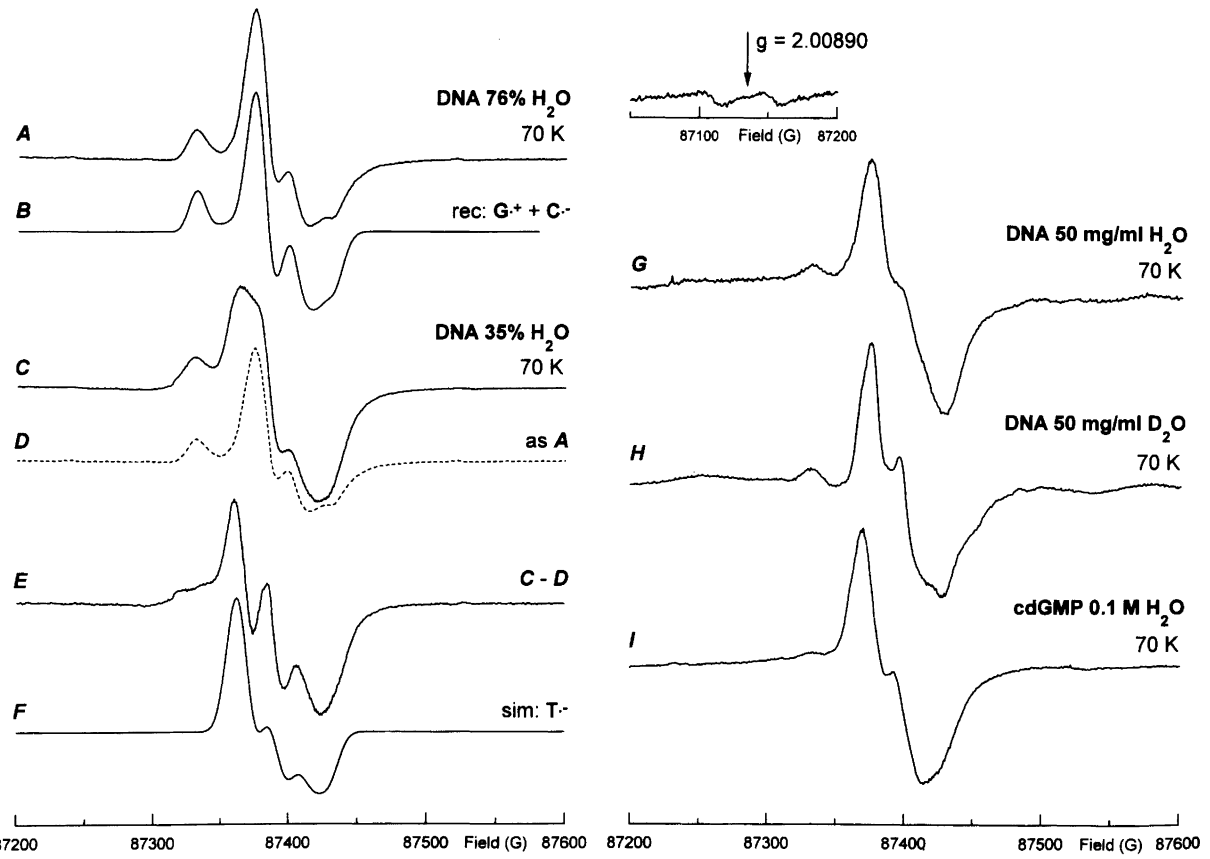

Fig. 4. ***A*** 245 GHz/8.7 T EPR spectrum of X-irradiated DNA equilibrated at 76% relative humidity in H_2O (cf., Fig. 3 ***D***) at 70 K. ***B*** Reconstruction of the spectrum in ***A*** using the simulated spectra of the guanine cation and the cytosine anion (cf., Fig. 1 ***D*** and ***F***) in about equal amounts. ***C*** 245 GHz/8.7 T EPR spectrum of DNA equilibrated at 35% relative humidity in H_2O (cf., Fig. 3 ***B***) at 70 K. ***D*** as ***A***, representation reduced to the magnitude at which ***D*** was subtracted from ***C*** to give ***E***. ***E*** Difference spectrum between ***C*** and ***D***. ***F*** The simulated thymine anion (cf., Fig. 1 ***H***) is given for comparison with ***E***. ***G*** 245 GHz/8.7 T EPR spectrum of X-irradiated DNA 50 mg ml^{-1} in H_2O at 70 K. Insert: doublet hyperfine lines of the ·OH radical at $g_\perp = 2.00890$. ***H*** as in ***G*** but in D_2O at 70 K. ***I*** 245 GHz/8.7 T EPR spectrum of X-irradiated cdGMP 0.1 M in H_2O at 70 K.

not yet possible since the component spectra in these matrices are still under investigation. Nevertheless, using the low-field line of $G^{\cdot+}$ as an indicator of its contribution and comparing the shapes of the spectra it becomes clear that there is a definitive shift of the contributing components in the frozen ice matrices compared, e.g., with 76% relative humidity which, among other things, decreases the contribution of $G^{\cdot+}$ considerably. This effect is even stronger in the frozen aqueous solution of cdGMP (spectrum ***I***) which was shown efficiently to stabilize $G^{\cdot+}$ in the dry state (cf. Fig. 1 ***A***).

Note that the temperatures of the frozen solutions were below the decay temperature of the hydroxyl radicals. This was proved by the presence of the doublet hyperfine lines at $g_\perp = 2.00890$ of ·OH (see the insert in spectrum ***G***).

Conclusions

The first results from high-field, high-frequency EPR studies on primary radical formation in randomly oriented DNA after X-irradiation at 77 K presented here give some unambiguous answers, showing the strength of the method in separating organic free radicals even with small differences in *g*-factors. Considering lyophilized powders equilibrated at different relative humidities, the presence of the guanine cation as an oxidized component has been proved beyond reasonable doubt. This species was characterized before mainly from inspection of oriented DNA fibers. Also, the cytosine anion can now be considered as a proven component, the contribution of which increases with increasing amount of water of hydration. Its previous descriptions came from either oriented DNA fibers in D_2O[12] or from frozen aqueous D_2O solutions.[9] For the first time, its presence in an H_2O environment has been ascertained in DNA. Likewise, the thymine anion, for a long time strongly assumed to be formed mainly due to the preponderance of its secondary H addition radical (structure **VII**) is now characterized in its own right.

Another question solved convincingly concerns the effect of water of hydration on the relative contributions of components. Under conditions of high field it is clear that the thymine anion contributes less with increasing

amounts of water of hydration. This explains the findings in oriented fibers in which, after replacement of thymine by deuteriated thymine, little effect was seen since the thymine anion is a minority species at 76% relative humidity.[7] The cytosine anion appears to be the preferred site of reduction in a strongly hydrated environment of DNA.

Finally, DNA in frozen aqueous solutions gives spectra differing strongly from those equilibrated in, e.g., 76% relative humidity. Specifically, the amount of guanine cation appears to be reduced considerably. This finding is in line with our proposal that the results of hydrated DNA and DNA in frozen solutions are different although the spectra at X-band frequencies show nearly no discernible differences.[9]

There are, however, new questions posed by our results. One is whether the components described above are all primary ones. This is difficult to answer. The intensity of response of a given component at X-band frequency may be different at the very high frequencies due to relaxation effects. It is one of the drawbacks of the present experimental set-up that the intensity of the laser cannot be adjusted over a sufficiently wide range to exclude saturation broadening. It is clear that for the components analyzed, this effect plays no role, however, and an inter-comparison is possible. This may not apply to other components. More work is needed in this direction once the set-up has acquired a Gunn diode as microwave source. For this reason, we have not given any quantitative estimates for the component contributions, e.g., in the reconstructions since they might be misleading.

Another question relates to the transfer of the simulated patterns at high fields to lower frequencies. It would be extremely rewarding to have more precise component characterizations available for work at X-band frequencies. This is, however, so far impossible. The spectra at 245 GHz are predominantly governed by the properties of the *g*-tensor elements. The hyperfine components rarely play a role since the experimental linewidths and, accordingly, the simulated linewidths are high. One may now, however, use the very precise knowledge of the *g*-tensor elements and combine this with precise hyperfine information to attempt new simulations of components at X-band frequencies.

Acknowledgements. This work was supported by a grant from BMBF (06 Ho 360).

References

1. Sevilla, M. D. and Becker D. In: Atherton, N. M., Davis, M. J. and Gilbert, B. C., Eds., *A Specialist Periodical Report—Electron Spin Resonance*, Vol. 14, Royal Society of Chemistry, Cambridge 1994, pp. 130–165.
2. Close, D. M. In: Charles, P.P. Jr., Ed., *Magnetic Resonance Review*, Vol. 11, Gordon and Breach, New York 1986, pp. 41–80.
3. Hüttermann, J. In: Lund, A. and Shiotani, M., Eds., *Radical Ionic Systems*, Kluwer, Dordrecht 1991, pp. 435–462.
4. Zell, I., Ph D thesis, Universität des Saarlandes (1990).
5. Gräslund, A., Ehrenberg, A., Rupprecht, A. and Ström, G. *Biochim. Biophys. Acta 254* (1971) 172.
6. Hüttermann, J., Voit, K., Oloff, H., Köhnlein, W., Gräslund, A. and Rupprecht, A. *Faraday Discuss. Chem. Soc. 78* (1984) 135.
7. Zell, I., Hüttermann, J., Gräslund, A., Rupprecht, A. and Köhnlein, W. *Free Radical Res. Commun. 6* (1989) 105.
8. Bernhard, W. A. *J. Phys. Chem. 93* (1989) 2187.
9. Sevilla, M. D., Becker, D., Yan, M. and Summerfield, S. R. *J. Phys. Chem. 95* (1991) 3409.
10. Cullis, P. M., McClymont, J. D., Malone, M. E., Mather, A. N., Podmore, I. D., Sweeney, M. C. and Symons, M. C. R. *J. Chem. Soc., Perkin Trans. 2* (1992) 1695.
11. Cullis, P. M., Evans, P. and Malone M. E. *Chem. Commun.* (1996) 985.
12. Gatzweiler, W., Hüttermann, J. and Rupprecht, A. *Radiat. Res. 138* (1994) 151.
13. Gregoli, S., Olast, M. and Bertinchamps, A. *Radiat. Res. 89* (1982) 238.
14. Symons, M. C. R. In: Fielden, E. M. and O'Neill, P., Eds., *The Early Effects of Radiation on DNA*, NATO ASI Series H 54, Springer, Berlin 1991, pp. 111–124.
15. Swarts, S. G., Sevilla, M. D., Becker, D., Tokar, C. F. and Wheeler, K. T. *Radiat. Res. 129* (1992) 333.
16. Lange, M., Weiland, B. and Hüttermann, J. *Int. J. Radiat. Biol.* 68 (1995) 175.
17. Hüttermann, J., Röhrig, M. and Köhnlein, W. *Int. J. Radiat. Biol. 61* (1992) 299.
18. Wang, W., Becker, D. and Sevilla, M. D. *Radiat. Res. 135* (1993) 146.
19. Mroczka, N. and Bernhard, W. A. *Radiat. Res. 135* (1993) 155.
20. Muller, F., Hopkins, M. A., Coron, N., Grynberg, M., Brunel, L. C. and Martinez, G. *Rev. Sci. Instrum. 60* (1989) 3681.
21. Dusemund, B. Ph D thesis, Universität des Saarlandes (1996).
22. Kim, H., Budzinski, E. E. and Box, H. C. *J. Chem. Phys. 90* (1989) 1448.
23. Close, D. M., Sagstuen, E. and Nelson, W. H. *J. Chem. Phys. 82* (1985) 4386.
24. Ohlmann, J. and Hüttermann, J. *Int. J. Radiat. Biol. 63* (1993) 427.

Received July 1, 1996.